Surface analysis and characterization of large printed-circuit-board circuitization process steps

by D. J. Auerbach C. R. Brundle

D. C. Miller

We describe our use of surface-analysis techniques to characterize problems encountered in 1980-1981 in the fabrication of large printed circuit boards for the IBM 3081 processor unit. XPS, AES, SAM, SEM, and optical microscopy techniques were used. The two major areas addressed were (a) corrosion at a photoresist/Cu foil interface during electroless Cu plating of circuit lines which resulted in defects in subsequently formed Cu lines, and (b) surface-chemical aspects of a "single-seed" colloidal Pd/Sn catalytic initiation of electroless Cu plating onto epoxy surfaces. The corrosion mechanism responsible for the line defects was identified, and corrective actions suggested. Changes in surface composition (Pd/Sn ratio), and surface chemical state (Pd⁰/Pd²⁺, Sn⁰ Sn^{2+,4+}) as a function of process step were correlated with plating effectiveness and led to a means of increasing the surface Pd⁰/Sn ratio by as much as an order of magnitude.

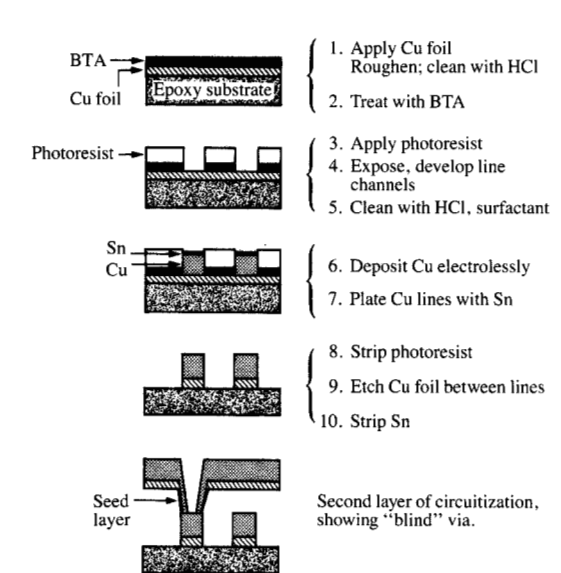
[®]Copyright 1988 by International Business Machines Corporation. Copying in printed form for private use is permitted without payment of royalty provided that (1) each reproduction is done without alteration and (2) the *Journal* reference and IBM copyright notice are included on the first page. The title and abstract, but no other portions, of this paper may be copied or distributed royalty free without further permission by computer-based and other information-service systems. Permission to *republish* any other portion of this paper must be obtained from the Editor.

1. Introduction

In 1980 a number of problems were encountered in the fabrication of printed circuit boards which were to be used in the IBM 3081 processor unit. The boards were relatively large (600 mm × 700 mm) multilayer printed circuit boards weighing 29 kg and contained a total of 20 layers, including six signal layers [1]. Nine pluggable thermal conduction modules (TCMs) were used to house the slightly under 1000 chips which were mounted on each board. This design, with a considerable number of internal connections, practically eliminated the need for traditional cable connections. Descriptions of the overall board technology can be found in [1]. Here we concentrate on the process steps used to form signal lines (circuitization process) and how the application of surface analysis and characterization was used to help overcome some associated fabrication problems.

In forming the signal layers, considerable use is made of processes involving lithography and electroless Cu plating. At the time this study was begun, photoresist-to-Cu-laminate adhesion problems had occurred during plating, resulting in subsequent circuitry defects (shorts, opens, and anomalies in line width or height). A review of the work in that area forms the first half of this paper. Another problem involved electroless Cu plating on the walls of through holes and "vias" connecting one level of circuitry to another. Pd/Sn colloidal "seeder" solutions are used to catalytically initiate that plating. We have investigated the surface chemistry

669



- 3. Apply T168 (du Pont) photoresist to the foil.
- 4. Expose the photoresist using a mask and remove (develop) unexposed resist, forming line channels.
- 5. Pre-clean the line channels (sequentially with dilute HCl, surfactant, water rinses).
- 6. Deposit 50 μm of Cu using an electroless plating process followed by rinsing and drying.
- 7. Plate the Cu lines with Sn for protection.
- 8. Strip the photoresist.
- 9. Etch away the thin Cu foil between the lines.
- 10. Remove the Sn.

This procedure resulted in the formation of a patterned layer containing Cu lines (the circuitry lines) which were 75 μ m wide and 50 μ m thick. Some explanatory comments are needed to clarify why some of the process steps were necessary. The purpose of the Cu foil was to provide an autocatalytic surface for the initiation of the electroless Cu plating. It subsequently had to be etched away (step 9), since its presence would lead to shorts. The T168 photoresist was

SIMILE

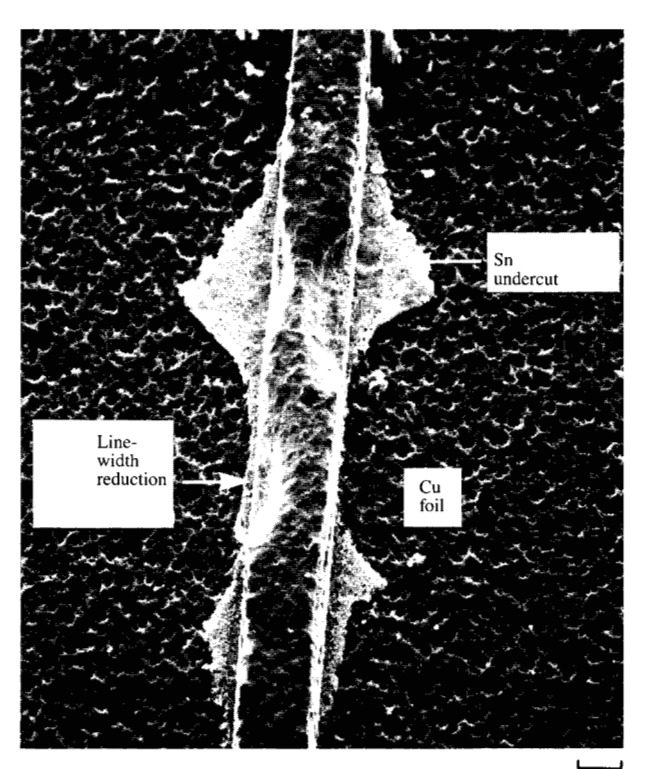
Schematic diagram showing relevant process steps used in signallayer fabrication.

associated with several variations of the seeding process. Some of this work, including laboratory simulations of the process and analysis of parts withdrawn from board fabrication at critical points, is reported in the second half of the paper.

2. Description of the process for forming a signal layer

Figure 1 shows a schematic diagram depicting major steps in signal-layer fabrication which were in use when this study was begun. Starting with a glass-reinforced epoxy dielectric substrate, the steps were as follows:

- Apply a thin Cu foil to the epoxy-glass surface and mechanically roughen the surface of the foil to improve adhesion of subsequently deposited layers.
- Treat the foil with Entek CU-56 (Enthone Inc., New Haven, CT), a commercial corrosion-inhibitor solution containing benzotriazole, m-nitrobenzene sulfonic acid, and methyl alcohol aqueously diluted from concentrate. [Hereafter, this is designated as the BTA (benzotriazole) treatment.]



50 ևո

Walter Trans

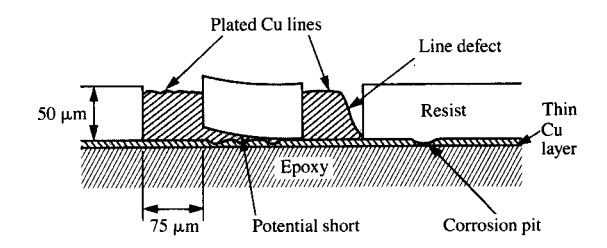
Scanning electron micrograph of a plated circuit line after step 8 of Figure 1, illustrating the two problems associated with resist delamination occurring during the Cu deposition stage (step 6): Sn was deposited not only on the Cu line, but also in "flares" on either side (Sn undercut); line-width reductions of the Cu line (the second problem) are apparent.

originally intended to be used directly on epoxy-glass surfaces. Its intrinsic adhesion to the Cu is poor, so the Cu had to be roughened to improve it. The BTA treatment is a widely used process for protecting Cu and Cu-containing surfaces from corrosion [2–5]. We have shown elsewhere [6] that the most effective processing parameters for the version of the treatment which was used produced about 30 Å of Cu-benzotriazole on the surface. The Sn plating process was used to protect the Cu lines during the etching which was used to remove the thin Cu foil.

3. Description of the signal-layer fabrication problem

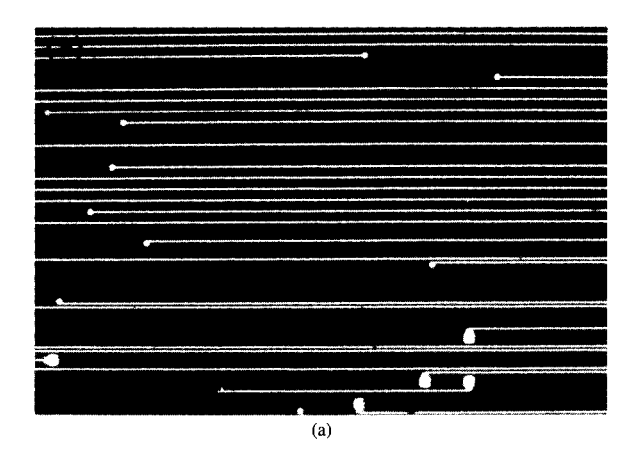
Functional difficulties of two types resulted from problems in the fabrication steps outlined above and were associated with an apparent photoresist adhesion problem. The first and most serious was "tin undercutting." For boards which exhibited a delamination of the photoresist next to the circuit lines, the Sn plating process (step 7) resulted in the deposition of Sn not only on the Cu lines, where it was needed, but also well to each side of the lines underneath the resist. Since areas covered by Sn were protected during the Cu etching (step 9), areas next to Cu lines where the Sn had penetrated were not etched away. The unetched Sn-covered Cu violated electrical specifications and led to a risk of shorts between lines. (See Figures 2 and 3.) The second problem, which was more ubiquitous than the Sn undercutting, was that the plated Cu lines adjacent to resist-failure regions did not have the desired uniform rectangular profile. Frequent line-width reductions and other defects occurred where Cu plating had apparently ceased locally and Cu was partially absent from the lines. This is also illustrated in Figures 2 and 3. Such lines did not meet dimensional specifications and could lead to failure during test cycling.

The difficulties described above were associated with apparent failures in photoresist adhesion. Figure 4(a) is a magnified photograph of a region of a board after it had been subjected to all the fabrication steps through the completion of the electroless Cu plating (step 6). The Cu lines had been plated to their full ~ 50 - μ m thickness and the resist, which was red, was still on the board. Figure 4(b) is a photograph of a board which exhibited widespread problems after the electroless plating process. In many places the resist adjacent to the plated lines appeared to be darkened, with black spots present within these regions. Examining the board with lighting at a grazing angle revealed that the resist was slightly bubbled above many, though not all, of the black spots. Of particular note was the very striking pattern dependence of the damaged regions. They were found only adjacent to Cu lines which were well spaced (greater than 1-3 mm) from other Cu lines. This pattern dependence was observed on all boards we examined that had damaged regions. Upon removal of resist from a damaged region, which could usually be achieved by flexing cutout sections of



E HITE

Schematic cross-sectional view through a signal layer after removal from the electroless plating bath (step 6). This illustrates the effects of corrosion and subsequent resist delamination.



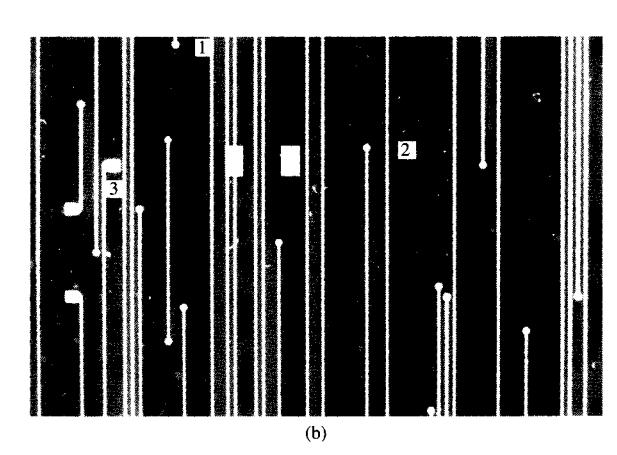


Figure 4

Photograph of portions of two circuit boards after completion of process steps up to and including electroless Cu plating, but before resist removal. The scale can be judged from the widths of the Cu plated lines, which are approximately 74 μm (see Figures 2 and 3). Photograph (a) shows a ''normal'' board. Photograph (b) shows Cu lines on a board exhibiting severe resist deterioration adjacent to Cu lines that are widely spaced from each other (see text).

the board a few times, the color of the removed resist was found to be actually the same as that of resist removed from undamaged regions. The apparent darkening observed with the resist on the board was actually a darkening of the Cu surface beneath the resist; the black spots were actually on the Cu surface. If an intact bubbled-resist region was sectioned through the bubbles, extensive amounts of foreign material were found in most, but not all, of the bubbles. Another visual observation of significance was that the black spots on the Cu surface were fairly regularly distributed. Their centers generally fell 0.6–0.8 mm from a plated line, and they never touched a line. Any proposed mechanism for the "resist failure" had to account for all the visual features described above, including the striking pattern dependence.

It is important to note that the line defects were correlated with the pattern dependence of the resist failure; i.e., they occurred more frequently and grossly on widely spaced lines than on closely spaced lines. It was not possible, in general, to associate the location of a particular defect with a particular black spot. However, where there was a higher density of black spots, there was a higher density of line defects.

4. Surface characterizations to establish the nature and mechanism of the fabrication problem

Resist failure at the electroless Cu plating stage had been a cause of concern from the start of the development of these types of board. It had been "contained" several times by varying parameters in several of the process steps prior to plating, and by the introduction of additional steps (e.g., mechanical roughening, which was introduced to counteract a smoother Cu foil supplied by vendors). None of these "containments" provided a permanent cure, since small changes in materials and process conditions could make the difference between "good" and "bad" performance. Factors known to influence the incidence of "bad" resist included the nature of the Cu foil surface as received (e.g., roughness, porosity, grain size), the details of the mechanical roughening process; the method of BTA surface treatment prior to resist lamination; the type of resist used; the exposure and development times during the lithography process; the length of delay between process steps; and the conditions in the plating bath itself (pH, temperature).

We started with the premise that the best chance for understanding the cause of the "black-spot" failure problem was to characterize the surface of the Cu foil after each process step. We hoped that these characterizations could also be used as control references for the process steps so that any subsequent changes could be detected. The analytic techniques we used in the black-spot studies were primarily X-ray photoelectron spectroscopy (XPS), Auger electron spectroscopy (AES), scanning Auger microscopy (SAM), scanning electron microscopy (SEM), and optical

microscopy. A full description of the results of the process step characterization is not given here; rather, we make reference only to those results which did, in fact, provide direct evidence on the nature of the black-spot problem.

The largest amount of helpful data came from examining the Cu foil/resist interface of a "bad" board after plating. Subsequently a set of boards with identical process history up to the plating stage were withdrawn from the plating process at times between initiation and achievement of the full plating thickness. Some aspects of the Cu foil/resist interface of these boards were also examined. In all cases resist was removed locally by a combination of flexing cutout sections of the board and applying pressure with a sharp point, causing large flakes of resist to delaminate. The revealed interface surfaces were then examined by one or more of the analytical techniques.

- Results on a "bad" board examined after plating

 On the basis of the pattern dependence of "bad" resist and black spots, we examined the Cu foil surface in three characteristic regions of the board:
- An area well away from all plated lines. We refer to this as an isolated area.
- An area between two Cu lines that are closely spaced, with no "bad" resist observed. We refer to this as a closely spaced line (CSL) area.
- An area adjacent to a Cu line with no close neighbor, and which had exhibited darkening, black spots, and bubbles in the resist before removal. We refer to this as a widely spaced line (WSL) area.

Examples of CSL and WSL areas are indicated as 2 and 3, respectively, in Figure 4(b).

Examination using SEM indicated that the surface topography of Cu foil in an isolated area was quite distinct from that of the plated Cu (Figure 5). Scanning electron micrographs of CSL areas showed a sharp demarcation between the plated Cu topography and the adjacent Cu foil topography. Scanning electron micrographs of WSL areas showed a more gradual change as one moved away from the plated lines. Given other data presented below, we believe this indicated that the Cu plating was taking place underneath the resist adjacent to widely spaced lines.

XPS data provide information on elemental and chemical state compositions within the first approximately 30-Å depth of the surface. At the time we took these data (1980, 1981), no small-spot XPS instruments existed, and the X-rays illuminated an area of approximately 0.05×0.5 cm. The results were, therefore, averages over that area. Near widely spaced lines, we were examining a region of the darkened Cu encompassing a number of black spots. The results of the elemental compositional analysis are given in **Table 1**.

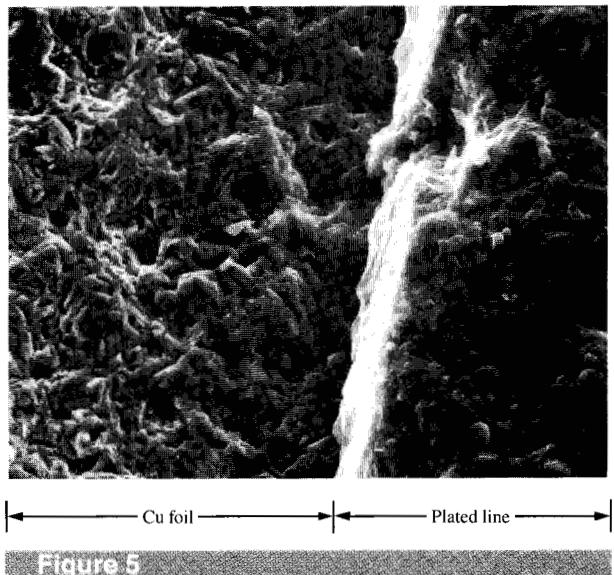
Chemical information is obtained in XPS by a detailed examination of the chemical shifts in binding energy (BE) and satellite structures associated with core-level transitions. In this study the features of importance that one can distinguish are (a) Cu²⁺ from Cu⁺, and (b) the nitrogen in benzotriazole from other forms of nitrogen on the surface, such as nitride, nitrate, etc. In fact, all the nitrogen observed on these surfaces was in the form of benzotriazole, since the N(1s) BE is at 399.6 eV, consistent with the value obtained for the BTA Cu⁺ complex formed by a controlled application [6] of BTA to Cu surfaces in our laboratory. It was also consistent with the value found on new parts examined immediately after the BTA application process (step 2). Examination of Table 1 reveals the following major qualitative points:

- In isolated regions the characteristic N(1s) signature of BTA was present at the intensity level found after initial application of BTA (step 2). The copper was present as a 50/50 Cu²⁺/Cu⁺ mixture. There was no evidence of any Na present.
- In CSL areas the level of BTA, judged by the N(1s) intensity, was reduced somewhat. The Cu²⁺/Cu⁺ ratio increased by a factor of two and Na was present.
- In WSL areas BTA was no longer present in detectable quantities, large amounts of Na were present, and the copper was almost entirely in the Cu²⁺ form.

Our conclusions from the XPS results were as follows. The presence of Na indicated that the Cu foil/resist interface had "seen" the NaOH of the plating bath. Since there was Na in both WSL and CSL areas, both regions had been penetrated, even though only the former produced "bad" resist. The complete removal of BTA in WSL areas, plus the fact that all the copper was in the Cu2+ form, suggested that a heavy oxidation or corrosion reaction had occurred. This was borne out by the SAM results of individual black spots, reported later. Thus, the gross resist delamination in WSL areas was either the result of oxidation/corrosion at the Cu foil/resist interface or it was the cause of the corrosion. We favored the former explanation, because whereas there were black spots under every resist bubble, there were black spots over which no resist bubbling had taken place; i.e., the oxidation/corrosion occurred before the resist bubbled.

SAM allowed us to look at regions of the surface with much finer spatial resolution than did XPS, but without its detailed chemical analysis capabilities. In particular, we could analyze areas within and adjacent to black spots.

Figure 6 is an absorbed-current micrograph taken with a scanning Auger electron spectrometer of a region of the Cu foil surface with two plated Cu lines. Three regions, indicated by arrows, were subjected to AES analysis: a CSL area (a), a black spot in a WSL area (b), and a region



Scanning electron micrograph of a portion of a board showing electroless plated Cu line and adjacent unplated Cu foil, illustrating the difference in morphology of the foil and plated regions.

Table 1 XPS-determined atomic compositions of Cu foil surface in regions indicated in Figure 4(b).

Region on board (see text)	Atomic composition*						
	Cu	0	С		Na (%)	Cu^{2+}/Cu^{+} , Cu^{0+}	
Isolated area (1)	4	23	69	4	0	0.5	
CSL area (2)	5	23	68	3	2	1	
WSL area (3)	5	23	67	0	5	>5	

^{*} Calculated from the XPS core-level peak areas corrected by the theoretical cross sections tabulated by Scofield [7], assuming a uniform distribution of the elements through the detection depth.

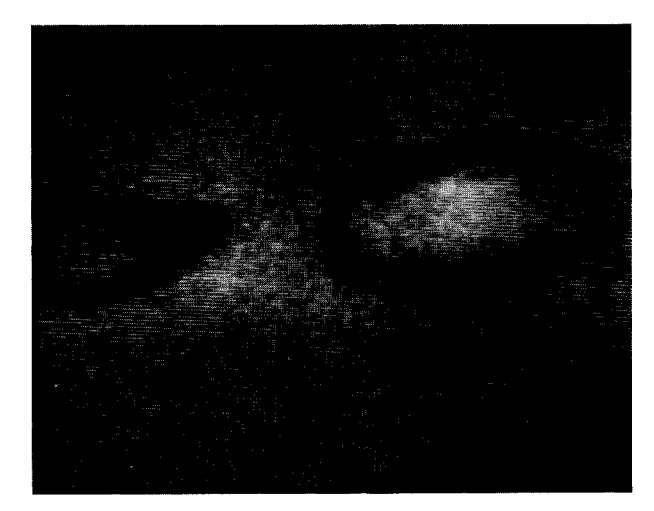
adjacent to that black spot (c). The elemental concentrations at the surface obtained from the Auger electron analyses are given in Table 2.

Two entries were made for each area analyzed: the "asreceived" results and a repeat analysis after a light (~20 Å) Ar⁺ etch of the surface. The absolute values cannot be compared directly to the XPS results of Table 1 because sampling depths vary depending on the kinetic energy of the signal being detected. This particularly affected the Cu values, since a rather low kinetic energy line is used in XPS (more limited to the surface), whereas the Auger kinetic energy is much higher (and therefore samples more deeply). Thus, a Cu surface contaminated with a foreign overlayer

It is possible to distinguish Cu²⁺ from Cu⁺ or Cu⁰ from the Cu 2p XPS features. It is not possible to distinguish Cu⁺ from Cu⁰, though this can be done by examining the X-ray induced copper AES lines.

Figure 6

Total absorbed current micrograph of area of board containing black spots, obtained using an Auger electron spectrometer. Regions for Auger electron analysis are marked. The scale may be judged from the plated lines, which are approximately 75 μm in width.



British.

Oxygen map of a black spot from Figure 6 using scanning Auger microscopy. Regions of highest oxygen concentration are the lighter regions.

Table 2 AES-determined atomic compositions of Cu foil surface in regions indicated in Figure 6.

Region on board	Atomic composition							
	Си	0	C (N (%)	Na	S	Cl	
Blank area	8.5	2.7	81	5.1	0	0	2.5	
Between lines (a) After light Ar ⁺ etching	23 54	13 23	51 17	3.3	3.7 3.5	5 2.7	0.2 0.4	
Black spot (b) After light Ar ⁺ etching	20 57	13 35	63 4.2	0 0	3 2.9	0.8 1.0	1.2 0	
Adjacent black spot	23	14	51	2.6	5	4.3	0.6	
(c) After light Ar ⁺ etching	58	22	12	0	5	2.1	0.4	

shows a much lower apparent Cu concentration in XPS than in AES, which is the case in comparing Tables 1 and 2. The significant results are that the trends observed in XPS were confirmed and additional information was provided concerning the individual black spots. The BTA nitrogen was completely absent only inside the black spots. Adjacent to them, in the rest of the WSL regions, a low level (lower than in the CLS area) was still present. In addition, the oxide in the black spots gave an indication of being thicker than in the areas adjacent to them, since the light Ar^+ etching, which removed the carbon contamination rapidly, revealed a greatly enhanced O Auger signal within the black spot. This

can also be observed in the SAM map of oxygen, taken after the light etch, shown in Figure 7. Oxygen was clearly concentrated in the spot. Equivalent carbon and Na maps showed that carbon was depleted in the black spots and that the Na had a uniform distribution over the whole area. Chlorine maps showed rather random distribution, with higher concentrations near the plated lines. Since chlorine is a common trace contaminant, we do not attach much significance to its distribution.

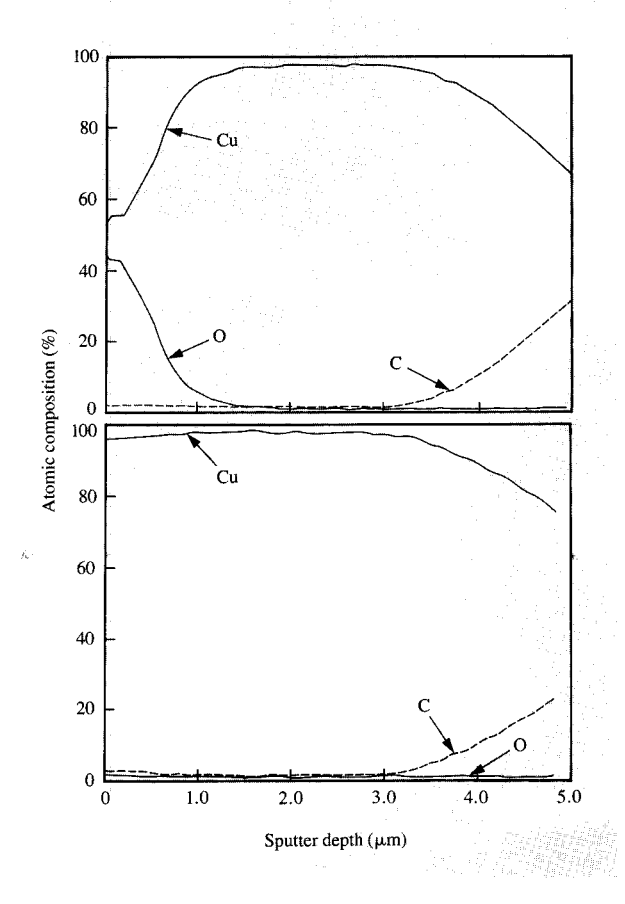
Since it appeared that there was a deeper oxide layer in the black spots than elsewhere, we depth-profiled through the 5- μ m thickness of the Cu foil in a black-spot region. The result, shown in **Figure 8**, was quite dramatic. The black spot was found to be oxidized to a depth of some 2 μ m, and was clearly a corrosion pit. Profiling adjacent to the black spot or in a CSL region showed that the contamination and oxide layers there were only of superficial thickness.

• Results on boards pulled from the electroless Cu plating bath at various times during plating

In this study, a set of boards which had been through the standard process sequence up to the Cu plating step were removed from the plating bath at 0.005, 0.013, 0.025, 0.05, 0.1, 0.15, 0.20, 0.25, 0.30, 0.40, 0.60, 0.70, 0.80, and 1.0 times the full plating time $t_{\rm p}$. They were immediately rinsed and examined with a light microscope, with the original intention of following the progressive conditions of resist and black spots. The darkened Cu regions and the initiation of black spots in the WSL areas began to become apparent only after 0.7– $0.8t_{\rm p}$ had been reached. By the end of plating, the

condition was much worse. The startling aspect of this visual analysis was that it was discovered that the penetration of the plating bath along the Cu foil/resist interface from the line channels could be observed quite easily, provided the boards were examined immediately. A uniform front progressing along both sides of all circuitry could be observed through the resist. After some time under the microscope (~1/2 h), the resist had darkened sufficiently that this phenomenon became difficult to observe. After spending only 0.005 of the required time in the plating bath, the front had penetrated approximately 25 μ m; after 0.025 t_p it had reached 75 μ m; after $0.10t_p$, $100-125 \mu$ m, with the front becoming more irregular. After $0.20t_p$ the front was at about 125 μ m, but that length of time in the plating bath had darkened the resist sufficiently that it was becoming difficult to see the front through it. Little further change could, therefore, be seen prior to the initial observation of darkened Cu at black spots in WSL areas at about $0.7t_n$. The conclusions from these visual observations are that penetration of the resist/Cu foil interface in the plating bath was immediate, that it occurred equally well adjacent to all lines (i.e., no pattern dependence) and that, for this particular set of boards, the penetration had reached about 125 μm in a macroscopic sense (i.e., visible by eye) after $0.1-0.2t_n$. That was already a sufficient distance for two fronts moving toward each other from adjacent closely spaced lines to meet, and free flow of the plating solutions had been achieved on a macroscopic scale. On the other hand, black spots and darkened Cu bands adjacent to widely spaced lines only appeared much later, at around $0.7-0.8t_n$.

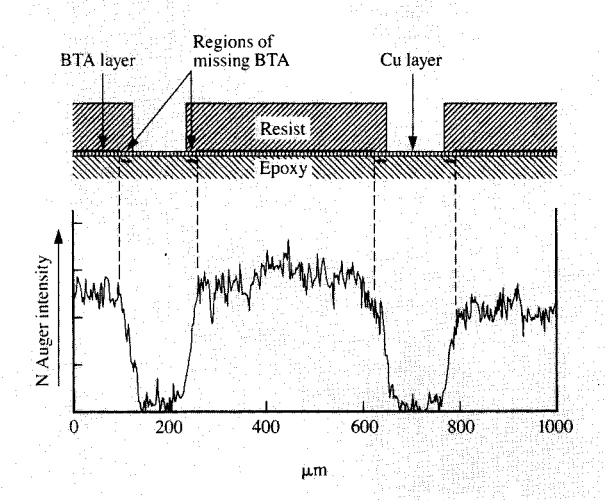
SAM analyses were carried out as a function of distance from line channels. The results for the $0.005-0.20t_p$ boards showed that Na concentration correlated well with visual observations of bath penetration. Na was detected within 25-50 µm of a plated line for the very early boards, and the contaminated area proceeded slowly out from the plated line. In addition, one could ascertain, from the N Auger electron signal, that BTA depletion from the surface correlated with the spread of the Na, suggesting attack of the BTA by the plating solution. Note, however, that the BTA concentration was only lowered, not eliminated, in agreement with an Auger electron analysis of a fully plated "bad" board (see the preceding subsection), where the BTA was found to be completely absent only inside black spots. One exception to this was very close to the line channels, where the BTA concentration was very low, even for the shortest time $(0.005t_n)$ in the plating bath. We had also analyzed a board immediately prior to plating, after step 5, the "line-channel preclean." The objective of step 5 was to remove all foreign material on the Cu foil at the bottom of the line channel after the lithography steps. This included the BTA on the Cu in this region. HCl is very effective in removing BTA, as we showed in a series of tests we performed on BTA-covered Cu to monitor its resistance to



Cu and O atomic concentration depth profiles of a black spot (upper curve) and of an isolated area of the Cu foil. The black spot was thus shown to be an oxidized area of considerable depth.

various environments. (Dipping a Cu surface, treated with BTA in a standard manner and having about 30 Å of Cu-BTA complex on the surface, into a beaker of cold 25% HCl for one minute removed about 85% of the complex.) The board, which had gone through "line-channel pre-clean" only, was stripped of its resist in a region containing several line channels, and a nitrogen Auger electron line scan was carried out across the region perpendicular to the line channels. The result is shown in Figure 9. BTA was absent in the line channels, as expected after the HCl pre-clean. Between lines the maximum concentration reached was consistent with that obtained from a surface freshly treated with BTA. Immediately adjacent to the line channels, however, the BTA concentration increased only gradually to the maximum value over a region of approximately 50 μ m. This was not connected with the lateral resolution of the spectrometer, since a spot size of only 1 μ m was used. The absence of BTA in this region signifies that the HCl pre-





Figure

Nitrogen concentration variation, measured using the N Auger signal intensity, in a line scan across the line channels of a board after the HCl cleaning procedure (step 5). To obtain this scan, the resist was removed from the board prior to analysis. The upper part of the figure shows how the line scan was geometrically associated with the channel regions. The lack of a nitrogen Auger signal indicated a lack of BTA. Note that the HCl cleaning removed BTA not only at the bottom of the line channels, but also in regions under the resist adjacent to the line channels (see text).

clean had itself penetrated the Cu foil/resist interface and attacked the BTA. Thus the corrosion protection for the Cu foil surface adjacent to the line channels was missing, and the Cu foil/resist interface was weakened even before the boards were subjected to plating.

5. Mechanism of black-spot formation and associated line-defect formation

From the discussion in Section 4 it is clear that the incoming pathway of the plating solution was along the Cu/resist interface from the line channels. We still need to explain the corrosion mechanism, the pattern dependence, and the correlation with the line defects. At first it seems paradoxical that one can have both *plating* and *dissolution* taking place on the same metallic surface, since the former involves Cu^{2+} reduction and the latter Cu oxidation. This paradox can be removed by considering the $[\operatorname{Cu}^{2+}]$ concentration gradients that might be expected under the resist. For plating to occur, the plating overpotential η must be negative,

$$\eta = E_{\rm p} - E_{\rm cq} = E_{\rm p} - \left(E^0 + \frac{RT}{2F} \ln \left[Cu^{2+}\right]\right),$$
(1)

where E_p is the electrochemical potential of the Cu surface, and E_{eq} is the equilibrium potential of Cu metal in the Cu²⁺ solution. As the plating solution moved along the Cu/resist

interface, plating will initially occur, since the bath is set up for η to be negative. Thus [Cu²⁺] will decrease continuously the further one moves from the line channel, once communication between the bath and the interface is sealed, or partly sealed, by the plating in the line channel. For isolated-line areas there is essentially an infinite sink; as diffusion continues, $[Cu^{2+}]$ will decrease until η becomes positive at some distance from the line channel, allowing a dissolution mode to ensue and corrosion to occur. Note that this is the same phenomenon as "crevice corrosion." For lines that are close enough together, [Cu²⁺] will not decrease enough for η to go positive and dissolution to occur before the solution meets a front moving from the opposite direction. In fact, we know that this meeting occurred within a short time, probably before the line channels were sealed, in which case [Cu²⁺] was essentially the same as in the bath.

This model explains most of the empirical observations concerning the resist failure. It explains the pattern dependence, and the fact that the black spots nearly always formed some significant distance from the lines and only after a long time in the plating bath. In addition, the resist lifting was always observed after the observation of the black spot. The beneficial role of the BTA, a well-known corrosion inhibitor, is explained, and it is clear that the BTA really was acting as a corrosion inhibitor, not an adhesion promoter. The general variability of the process could then be understood to be due, at least in part, to poor control over the BTA application process, and particularly the environmental conditions and delays between application and resist lamination. Finally, the detrimental effect of high pH in the plating bath is understood in terms of increased corrosion under more caustic conditions.

What we have not explained, so far, is the correlation of the resist failure to the formation of the line defects. We believe this was due to the transport of some of the large amount of debris and hydrogen resulting from the corrosion process at the black spot back to the vicinity of the line channels, where it inhibited plating locally. In fact, in a simulated plating bath set up where direct videotaping was possible, gas bubbles were observed to escape at the line channels during plating. I

6. Solutions to the signal-layer fabrication problem

Clearly the poor adhesion quality of the T168 resist/Cu foil interface, which allowed rapid penetration of plating bath solutions so easily, was the major culprit. It was possible, by simultaneously making improvements in several aspects of the process, to increase the yields greatly while retaining the T168 resist/Cu foil interface.

If one accepts that plating-bath penetration of the interface is always a possibility, it is necessary to eliminate,

Roy Magnuson, IBM Endicott, private communication.

or reduce, the conditions which favor corrosion under such circumstances. A major effect on this is the quality of the Cu BTA complex 30-Å-thick layer which was introduced in order to inhibit corrosion. The proper application of the BTA was important in this respect. Preparing the surface initially with a thin oxide (e.g., by immersion in nitric acid or sodium carbonate), proper concentration of the BTA, and proper temperature were shown to be important [6]. Furthermore, two factors limited the effectiveness of the BTA protection. First, there were long delays (sometimes weeks or months) between BTA application and resist lamination, with the BTA-treated boards stored in uncontrolled and sometimes potentially hostile environments (e.g., near HCl cleaning baths). Instituting environmental control and immediate resist application after BTA treatment helped considerably. Second, the linechannel pre-cleaning step prior to plating was removing BTA adjacent to the line channels. It was shown that more benign conditions still provided effective line-channel cleaning and that this would represent a possible further improvement to the process.

Improvements in control of the lithographic process steps were also made which considerably improved the adhesion at the T168 resist/Cu foil interface, thus helping further to alleviate the black-spot problem. Basically, the UV exposure step which was used to cure (cross-link) the resist was erratic and led to overexposure and embrittlement at the bottom of the resist. Finally, improvements could be made in the plating bath itself so that a faster rate of plating could be achieved and the boards would not have to spend as long in that hostile environment. Although penetration of the interface occurred within a few minutes, the corrosion problems did not materialize until after about 0.8 of the full plating time had elapsed.

7. Pd/Sn seeding processes for initiation of electroless Cu plating on insulators

Although Cu foil was used to initiate plating of the circuit lines, there were still bare-epoxy regions of the board that needed to be electrolessly plated during the deposition of subsequent layers of circuitization. These regions were the holes drilled through the board for the pin connections of the TCMs and the "blind" vias (Figure 1) connecting one layer of circuitry and the next, as discussed in [1]. To initiate Cu plating directly on epoxy, it was necessary to pretreat the surface with a "seeder." There are a variety of seeding methods which can be used, including (1) the "double-seed" process, where the major steps are sequential immersion in acidic SnCl₂, then acidic PdCl₂ solutions; and (2) the "singleseed" process, in which a dip into a colloidal suspension made from a mixture of PdCl, and SnCl, in HCl is used. In the scientific literature, the double-seed process is more commonly known [8-11] as sensitization (SnCl, dip) and activation (PdCl₂ dip), whereas the single-seed process is

known as the mixed catalysis [12–16] process. At the beginning of our involvement in this work, another process was in use which consisted of double-seed followed by single-seed; this was termed the "triple-seed" process. With improved understanding and control, leading to greater seeding efficiency, the triple-seed process was replaced by the single-seed process for initiating plating in vias and through holes.

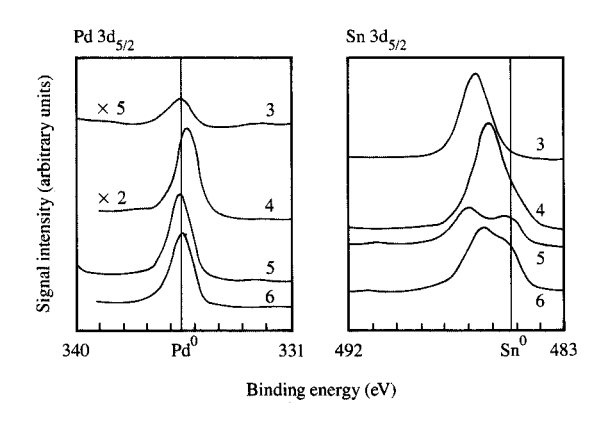
In the following sections we briefly describe the surface studies we performed to characterize the surface chemistry of the single-seed process and the improvement we were able to make to it with this knowledge. The details of the double-seed process are reported elsewhere [17]. In addition, we describe an experiment where, using surface-analytical techniques, we were able to explain why in a particular fabrication sequence the triple-seed process worked, whereas the single-seed did not, even though many other tests had shown the single-seed process to be an acceptable seeding process.

The single-seed, or mixed-catalysis, process was first suggested and patented by Shipley [12]. In that patent he claimed that colloidal Pd/Sn particles, deposited on the insulating surface, acted as Cu plating nucleation sites. The exact nature of the particles has, however, been the subject of controversy. It is unclear whether the particles are a true Pd/Sn alloy (Pd₃Sn has been suggested) [11] or a mixture and, whereas one might intuitively think the Pd in a Pd/Sn alloy is the active catalytic site, it has been suggested that a colloidal particle with a Pd/Sn core surrounded by a stabilizing layer of Sn²⁺ is the active species [15]. The singleseed process is actually not a one-step process, as its name might imply. The catalysis step is usually followed by an "acceleration step" which enhances the activity of the colloidal particles toward plating. Ammonium fluoroborate, ammonium bifluoride, hydrochloric acid, sulfuric acid, and sodium hydroxide have all been used as accelerators. There are several surface-analytic studies reported which suggest [16, 18-20] that the "accelerator" removes Sn from the surface of the particles, thereby increasing the Pd/Sn ratio. Below we report our surface studies of several versions of the single-seed process.

8. Surface composition and chemistry of seeder particles during single-seed processing steps

The single-seed process in use at the time our investigations of seeding were begun consisted of the following steps:

- 1. Clean board with hot detergent.
- 2. Rinse board with hot de-ionized water.
- 3. Immerse board in a commercial single-seed colloidal solution for three minutes.
- 4. Rinse in de-ionized water for one minute.
- 5. Immerse board in 1 M HCl at room temperature for one minute. This step was termed acceleration.
- 6. Rinse board in de-ionized water for one minute.



Faure 10

Pd and Sn X-ray photoelectron spectra of epoxy substrate after the indicated steps in the single-seed process: 3, immersion in single-seed solution; 4, first rinse; 5, HCl acceleration; 6, final rinse. The elemental concentrations are proportional to the signal intensities, and the chemical state can be determined from the measured binding energies (see text).

Table 3 Atomic composition (%) of single-seeded epoxy surfaces as determined by XPS.

After seeding	Stan	dard single process	5 mM NaOH process			
		After DI rinse	After 1 M HCl	After DI rinse	After NaOH and DI rinse	
Pd	0.4	4.1	8.3	8.2	6.8	10.1
Sn	10.9	20.7	10.3	12.3	1.4	2.5
0	12.8	29.3	8.5	25.8	23.8	10.2
Cl	25.4	2.3	11.2	3.7	_	_
F	18.1	_				_
C	25.8	43.6	61.6	50.0	72.9	77.2
S	1.4	_		_		
Na	5.3	_			5.9	_

We set up a laboratory-scale line to carry out this process on small glass-reinforced epoxy substrates, and at each stage of the process took samples from this mini-line, dried them with house nitrogen, and subjected them to XPS analysis. The concentrations of the various elements observed on the surfaces are given in **Table 3**. They are calculated from peak intensities using the same assumptions made earlier in the black-spot study. As in that study, we could use the experimentally determined BEs to tell us something about the chemical state of the elements present. In particular, we could distinguish Pd⁰ from Pd²⁺, because there is about a 2-eV difference in the Pd 3d binding energy of these two chemical states [21]. Similarly, we could distinguish Sn⁰ from Sn^{2+/4+} by a 1.5-eV difference in the Sn 3d_{5/2} peaks [21].

We could not, however, distinguish Sn^{2+} from Sn^{4+} , since their BEs are identical to within 0.2 eV [21]. Some regions of the actual spectra used to obtain the numbers in Table 3 are shown in **Figure 10**.

Looking at Table 3 and Figure 10, we can see that after the initial immersion in seeder (step 3), only a very small amount of Pd (which was in the metallic Pd⁰ state) was observable within the probing depth (~30 Å) of the analysis. There was an amount of Sn 25 times greater, all of it in the oxidized Sn²⁺ or Sn⁴⁺ state. The large carbon signal arose mainly from the epoxy substrate. The chlorine (in the form of Cl⁻ from the observed BE) arose from the Cl⁻ counterions of the colloidal particle complex. The F⁻ was initially a surprise to us, but we later learned that a fluorocarbon wetting agent is an additive to the commercial seeding solution. Sulfur and sodium were ubiquitous contaminants.

After the DI rinse (step 4) the fluorine, sulfur, and sodium signals were gone and the chlorine signal reduced dramatically. Consequently, all the other signals increased. The Pd/Sn ratio, however, increased by a factor of 5, and the Sn 3d_{5/2} peak position suggested that some of the Sn observed was in the metallic form (Figure 10). The acceleration step (5) increased the amount of Pd⁰ by a factor of two, decreased the amount of Sn by a factor of two, and replaced oxygen counter-ions with chloride. The Sn within the probing depth was roughly 50/50 metallic/oxidized. The final rinse (step 6) replaced chlorine with oxygen again, but changed little else.

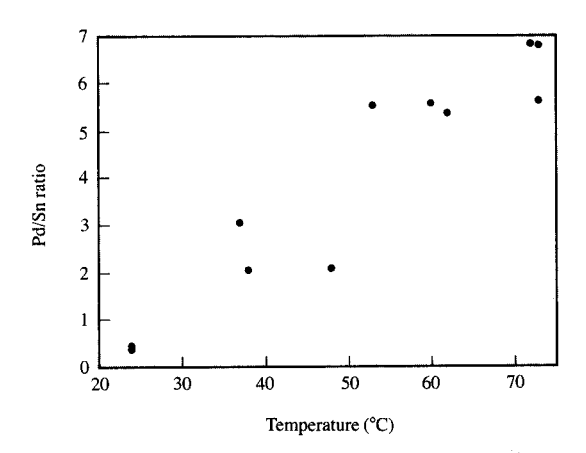
The above results, together with the previous work [16, 18-20, 22, 23] in the literature, led us to the following mechanism for the single-seed chemistry. After the seeding step, a layer of particles containing Pd and Sn in their metallic states is deposited. The outer sheath of these particles consists of Sn chloride, oxide, and hydroxide, plus fluoride contamination. From subsequent studies [24] of oxidation of Pd/Sn alloys under controlled conditions, we know that thermodynamically it is highly favorable for Sn to segregate to the surface and form tin oxide, so it is not surprising that in these colloidal deposited particles the outer sheath should have Sn in the oxidized form present and very little Pd present. The DI rinse removes the contaminants and soluble tin chloride. Since some of the outer sheath is thus removed, XPS "sees" further in; hence the rise in the Pd/Sn ratio and the observation of a small amount of Sn^o. The HCl acceleration step then dissolves away most of the Sn oxide/hydroxide sheath, exposing more of the particle core and therefore increasing the Pd/Sn ratio. The surface Sn is also converted to tin chloride again. The final rinse removes the Sn chloride and leaves an equivalent amount of Sn oxide/hydroxide. Thus, the whole process has had the effect of largely stripping off the thick (≫30 Å) layer of oxidized tin. This mechanism is largely in agreement with the one proposed by Cohen and West [15], where they

showed using Mössbauer spectroscopy that the seeder particles are composed of Sn/Pd (presumably as an alloy), surrounded by a layer of $\mathrm{Sn^{2+}}$ ions. In addition to detailing the surface changes at each step, our surface studies showed that though the HCl accelerator causes the stripping of oxidized Sn from the seeder surface, it is not entirely effective at this. The surface $\mathrm{Pd^0/Sn}$ ratio is only ~ 0.7 , whereas the bulk Pd/Sn ratio is ~ 3 . We further demonstrated that the seeder particles are still very rich in tin oxides at the surface after acceleration by subjecting them to $in \ situ \ \mathrm{Ar^+}$ sputtering and then re-analyzing. After a brief sputtering the Pd/Sn ratio did approach 3.

Our earlier work on the double-seed process [17] showed that there was a direct correlation between the surface Pd⁰ concentration and subsequent plating activity. We therefore expected that the Pd⁰ of the single-seed particles would be the catalytically active component and that the activity of the seeder should improve with higher Pd⁰ concentration. To first order we knew that this was true, since the unaccelerated seeder, with a very low Pd⁰ concentration at the surface, is not very effective in initiating Cu electroless plating. Since we also knew that the standard process, including HCl acceleration, still left the Pd/Sn ratio at the surface a factor of ~4 lower than the bulk value, the question arose as to whether there are modifications that could be made to the processing to improve the surface Pd/Sn ratio.

One way to try increasing the seeder activity, since we believed it was the *surface* Pd⁰ concentration that was important, was to find a more effective accelerator for stripping the tin oxide sheath from the seeder particles. We determined the surface composition of standard singleseeded substrates treated with a variety of accelerators and accelerating conditions. After HCl acceleration, the surface composition was found not to be strongly dependent on acceleration time (1 to 10 minutes), concentration (1 M to 6 M), or temperature (28°C to 73°C). Acceleration with either 1 M NaOH or 1 M H₂SO₄ gave an end result of less Pd, less Sn, and more carbon than the HCl treatment. Apparently these accelerators, under the above conditions, remove seed particles entirely from the surface in addition to stripping the Sn sheath. The Pd/Sn ratio did increase from ~0.7 to ~1.0 for these accelerators, however.

The above accelerating conditions have been reported previously [16, 19, 20, 25]. We have found that acceleration using hot, dilute NaOH gives quite different seeder surface-composition behavior than any of the above processes [26]. The results for 0.005 M NaOH at 73°C are given in Table 3. The major effect was to dramatically reduce the surface Sn concentration, thereby increasing the Pd/Sn ratio to about 5. The Pd 3d XPS spectrum indicated, however, that this surface Pd was divided about equally into Pd⁰ and Pd²⁺. Since we believed it was the Pd⁰ that was effective in the catalytic initiation of plating, we wanted to reduce the Pd²⁺



E TITTO

Surface Pd/Sn ratio (determined by XPS) for single-seeded epoxy substrates accelerated with 5 mM NaOH for three minutes as a function of temperature. An improvement of more than an order of magnitude was obtained at 73°C, compared to the standard single-seed acceleration process (see text).

to Pd⁰. We were able to do this with a subsequent formaldehyde rinse (0.074% at 73°C). The Pd⁰/Sn ratio was about 4 after this treatment (Table 3). In a later series of experiments, we subjected a set of samples (which had been processed simultaneously) to acceleration with dilute NaOH process at temperatures between 23°C and 73°C. The resulting Pd/Sn ratios are shown in Figure 11. It is clear that there was a direct correlation between temperature and the Pd/Sn ratio, with a maximum of nearly 7 being reached at 73°C for that particular set. This is to be compared to the value of ~0.7 for the standard single-seed process.

Our understanding of the surface chemistry of the singleseed process was put to use when a problem arose soon after changes were made in the process for seeding vias and through holes. Two changes were made simultaneously: the seeding process was changed from triple-seed to single-seed, and the temperature of the BTA process was increased. Plating voids were found in the vias of boards that had been single-seeded, while triple-seeded boards plated normally during fabrication of the second layer of circuitization. Available data suggested that the problem was related to exposure to the hot BTA process. We subjected epoxy-glass substrates to single-seeding, put them through the chemical steps of the benzotriazole process (25% HCl, Na₂CO₃, 60°C BTA), and analyzed them. XPS analysis indicated that the HCl and Na₂CO₃ acted as accelerators, removing Sn from the seeder surface; the Na₂CO₃ partially oxidized the exposed Pd, and the BTA left a nitrogen-containing film on the

Table 4 XPS-determined atomic compositions of epoxy surfaces after seeding, air bake, and exposure to the BTA process (see text).

Seed process	Atomic composition							
	C	0	N		Sn (%)	Pd/Sn	Pd ⁰ /Pd	
Standard single-seed (HCl accelera- tion)	62	15	10	7.8	5.0	1.6	~0.3	
Single-seed without HCl acceleration	68	17	2.6	4.9	7.4	0.66	1	
Standard triple-seed (no HCl acceleration)	51	33	3.2	3.5	9.3	0.38	1	
Triple-seed with HCl acceleration added	59	31	4.6	1.7	4.4	0.39	~0.3	

surface. Microprobe analysis² indicated that the 25% HCl and Na₂CO₃ also removed seeder in bulk. The damage done by exposure of the single-seeded samples to the hot BTA process was therefore threefold—bulk loss of seeder, oxidation of the active palladium sites, and coverage of seeder sites by a BTA residue/complex.

These results explained the failure of the single-seed process in the presence of the BTA process, but did not explain how triple-seeded parts had historically survived. After all, the last major step of the triple-seed process was a dip into the single-seed solution. Closer examination showed one significant difference in the treatment of single-seed and triple-seed parts after the dip into the colloidal solution; the single-seed parts were accelerated with 8% HCl, while the triple-seed parts were not. All the boards were baked at the end of the seeding process. To test the hypothesis that the exposure to HCl before drying and baking was the key factor, we performed an experiment in which four procedures were compared: standard single-seeding (with HCl), single-seeding without the HCl step, standard tripleseeding (with no HCl), and triple-seeding with HCl added. Table 4 summarizes our results. XPS analysis of nonaccelerated, baked single-seed samples after exposure to the BTA process showed the palladium to be present as all Pd⁰. Only a small nitrogen signal was observed, indicating that there was less BTA residue on the surface. Conversely, when triple-seed parts were accelerated with 8% HCl before the bake and before the BTA process, the surface palladium was partially oxidized. Standard triple-seed parts (no acceleration) showed the palladium as all Pd⁰, with less surface nitrogen than triple-seed parts that were accelerated before the final bake.

Our conclusions from our work on the single-seed process are as follows:

- The Pd/Sn seeder is initially deposited as a metallic Pd-Sn core, surrounded by Sn in a higher oxidation state and several types of counter-ions. The DI rinse removes and hydrolyzes the tin chloride present. The accelerator process serves to remove the remaining oxidized tin layer, though not always very effectively.
- Hot dilute NaOH is an excellent accelerator, increasing the surface Pd/Sn ratio by up to a factor of 10 over the standard process. Any oxidation of the Pd can be reversed by treatment with formaldehyde solution.
- HCl acceleration of the mixed-catalysis seeder before baking leaves the surface of the core Pd/Sn particle vulnerable to chemical and physical attack from subsequent treatments such as the BTA process.

9. Concluding remarks

Surface-analysis techniques have proven to be very valuable in the study of problems encountered in the fabrication of printed circuit boards. Successful fabrication of such boards has come to depend increasingly on understanding and characterizing associated surface phenomena. We have shown how problems associated with a corrosion inhibitor only a few monolayers thick could lead to board-fabrication problems, and how critical the chemical state of the surface of catalytic seeder particles could be to the proper functioning of the processes with which they were associated. A step-by-step characterization of processes was proven useful, not only from the point of view of understanding and optimizing the processes, but also to provide diagnostics of which steps were at fault when problems arose.

Acknowledgments

Throughout the nearly five years during which this work was carried out, we received constant encouragement and

On the basis of our understanding of the single-seed process, we postulated that the bake before acceleration fully oxidizes the Sn coating of the seeder, making it resistant to attack by HCl and protecting the active seeder core. Accelerating the seeder partially removes the outer Sn layer, leaving the palladium in the seeder core vulnerable to oxidation and complexation with the BTA nitrogen. Coupon-plating experiments were carried out in the Endicott development laboratory tanks to see if the plating take would follow our surface-analytic results. Single-seed and triple-seed samples without acceleration prior to bake initiated plating well after going through the hot BTA process; samples accelerated before bake, single- or tripleseeded, showed poor plating initiation. These results confirmed our hypothesis for the mechanism for the singleseed failure in the presence of BTA, and added understanding of the nature of the seeder itself.

² T. Huang, IBM Almaden Research Center, private communication.

support from D. P. Seraphim. Without his willingness to hear us out on both finicky scientific detail and difficult policy or organizational issues, our contributions in this area would not have been possible. Many other colleagues from the System Products Division at Endicott, New York, and from the IBM Research Division contributed in important ways to the work described in this paper. It is impossible to list them all, but their help is gratefully acknowledged. We would like particularly to thank J. G. Gordon III for important contributions to the early phases of this work, P. A. Alnot for important contributions to the work on seeding, and W. Alpaugh, D. Barr, D. Jung, R. Magnuson, V. Markovich, R. Mead, and R. Parsons for stimulating discussions, help in obtaining critical samples and materials, and collaborative work on various phases of this study.

References

- Donald P. Seraphim, IBM J. Res. Develop. 26, 37 (1982); for a description of associated process steps, see Principles of Electronic Packaging Design and Materials Science, D. P. Seraphim, R. C. Lasky, and C. Y. Li, Eds., McGraw-Hill Book Co., Inc., New York; to be published mid-1989.
- 2. Proctor and Gamble, Ltd., British Patent 652,339, 1947.
- 3. G. W. Poling, Corros. Sci. 10, 359 (1970).
- 4. R. Walker, J. Chem. Ed. 57, 789 (1980).
- 5. D. Chadwick and T. Hashemi, Corros. Sci. 18, 39 (1978).
- D. C. Miller, D. J. Auerbach, and C. R. Brundle, Research Report RJ-3917, IBM Research Laboratory, San Jose, CA, 1983.
- 7. J. H. Scofield, J. Electron Spectrosc. 8, 129 (1976).
- J. P. Morton and M. Schlesinger, J. Electrochem. Soc. 115, 16 (1968).
- 9. R. Sard, J. Electrochem. Soc. 117, 864 (1970).
- R. L. Cohen and K. W. West, J. Electrochem. Soc. 119, 433 (1972).
- N. Feldstein and J. A. Wiener, J. Electrochem. Soc. 120, 475 (1973).
- 12. C. R. Shipley, Jr., U.S. Patent 3,011,920, 1961.
- 13. E. D. D'Ottavio, U.S. Patent 3,532,518, 1970.
- 14. A. Rantell and A. Holtzmann, Plating 61, 326 (1974).
- R. L. Cohen and K. W. West, J. Electrochem. Soc. 120, 502 (1973).
- T. Osaka, H. Nagasaka, and F. Goto, J. Electrochem. Soc. 127, 2343 (1980).
- P. Alnot, C. R. Brundle, D. J. Auerbach, and D. C. Miller, Research Report RJ-4710, IBM Research Laboratory, San Jose, CA, 1985.
- 18. R. L. Meek, J. Electrochem. Soc. 122, 1177 (1977).
- T. Osaka, H. Takematsu, and K. Nihei, J. Electrochem. Soc. 127, 1021 (1980).
- J. J. Grunwald, S. Gottesfeld, and D. Laser, *Plating* 68, 71 (1981).
- 21. K. Holm and S. Storp, Appl. Phys. 9, 217 (1976).
- R. L. Cohen, J. F. D'Amico, and K. W. West, J. Electrochem. Soc. 118, 2042 (1971).
- 23. R. L. Cohen and R. L. Meek, Plating 63, 47 (1976).
- H. H. Rotermund, V. Penka, and C. R. Brundle, J. Vac. Sci. Technol. 5, 1198 (1987).
- 25. R. L. Cohen and R. L. Meek, U.S. Patent 4,042,730, 1977.
- P. R. Alnot, D. J. Auerbach, C. R. Brundle, and D. C. Miller, U.S. Patent 4,640,718, 1987.

Received February 5, 1988; accepted for publication June 15, 1988

Daniel J. Auerbach IBM Research Division, Almaden Research Center, 650 Harry Road, San Jose, California 95120. Dr. Auerbach is the manager of the Physical Sciences Department at the IBM Almaden Research Center. He received his Ph.D. from the University of Chicago; before joining the IBM San Jose Research Laboratory in 1978, Dr. Auerbach held research positions at the FOM Institute, Amsterdam, and the University of Chicago, and served on the faculty of the Johns Hopkins University. His research interests center on the dynamics of gas-surface interactions, including the determination of potential energy surfaces, the study of energy transfer processes, and the investigation of the detailed mechanisms of chemical processes on surfaces. (Molecular-beam and laser-spectroscopic techniques are used to allow quantum-state-specific studies of the microscopic details of fundamental gas-surface-interaction processes.)

C. R. Brundle *IBM Research Division, Almaden Research Center, 650 Harry Road, San Jose, California 95120.* Dr. Brundle is the manager of the Micro, Surface, and Analytical Science Department, within the Physical Sciences Department at the IBM Almaden Research Center. He received his Ph.D. from Imperial College, London University, and joined the IBM San Jose Research Laboratory in 1975. Before joining IBM, Dr. Brundle was a member of the chemistry faculty at Bradford University, England. His research interests center on the use of electron spectroscopies and other surface-sensitive techniques for surface electronic structure and characterization studies. A major area of activity has been the interaction of oxygen with metal and alloy surfaces. He is the editor of the *Journal of Electron Spectroscopy*.

Dolores C. Miller IBM Research Division, Almaden Research Center, 650 Harry Road, San Jose, California 95120. Ms. Miller is a staff scientist in the Micro, Surface, and Analytical Science Department, within the Physical Sciences Department at the IBM Almaden Research Center. She joined the IBM San Jose Research Laboratory in 1975. Ms. Miller received her A.B. from Bryn Mawr College, Pennsylvania, and her M.S. from Stanford University, California, both in chemistry. Her current research interest is applied X-ray photoelectron spectroscopy. In 1987 Ms. Miller received an Outstanding Technical Achievement Award for her work on seeding processes for printed circuit boards.